CRYSTAL GROWTH & DESIGN
pubs.acs.org/crystal
Article

Nonmetallic Pentazole Salts Based on Furazan or 4-Nitropyrazole for Enhancing Density and Stability

Wei Hu, Hongwei Yang, Jieyi Chen, Chong Zhang, Chengguo Sun, Bingcheng Hu,* and Guangbin Cheng*

Cite This: *Cryst. Growth Des.* 2021, 21, 2690−2698

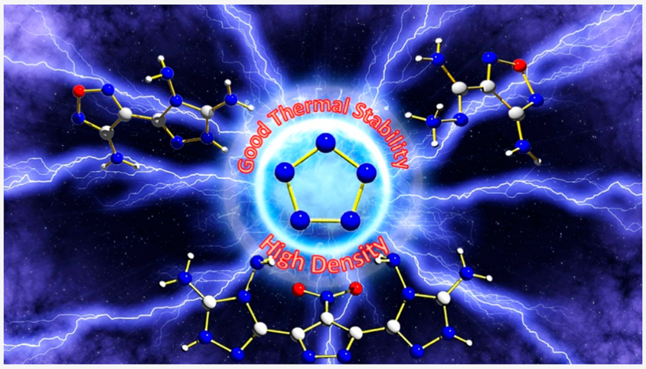

ABSTRACT: In this work, three novel nonmetallic pentazole salts (**6**−**8**) based on furazan or 4-nitropyrazole were synthesized. Some coplanar groups were introduced into the compounds to improve the planarity of the crystal packing. 4-Amino-1,2,5-oxadiazole-3-carbohydrazonamide pentazolate (**6**), 5-(4-amino-1,2,5-oxadiazol-3-yl)-4*H*-1,2,4-triazole-3,4-diamine pentazolate (**7**), and 5,5′-(4-nitro-1*H*-pyrazole-3,5-diyl)-bis(4*H*-1,2,4-triazole-3,4-diamine) pentazolate (**8**) all show more stable $\pi-\pi$ stacking and exhibit superior thermal stability (110.5−116.4 °C) than most other reported nonmetallic pentazole salts (T_{onset}: 80−110 °C), and compound **8** has the highest crystal density (1.722 $g \cdot cm^{-3}$/173 K) of nonmetallic pentazole salts to date. All salts have been thoroughly characterized by NMR (^1H and ^{13}C) spectroscopy, infrared (IR), Roman (RA), and elemental analysis. The decomposition temperature of all salts displays more than 110 °C, which is measured by differential scanning calorimetry (DSC). These compounds all shows low sensitivity (IS > 35 J, FS > 360 N) measured by standard BAM methods. Glycidyl azide polymer (GAP) based propellant formula with the addition of salt **6** or **7** shows a higher specific impulse (**6**, I_{sp} = 262.1 s; **7**, I_{sp} = 263.9 s) than that of RDX (I_{sp} = 259.0 s). This study can provide a new crystal engineering way for the synthesis of pentazole salt to solve the problem of low density and poor stability.

■ INTRODUCTION

Polynitrogen compounds have received great attention due to their great potential as high-energy-density materials (HEDMs).[1−3] In 1956, Huisgen and Ugi first addressed the issue of aryl pentazole ($Ar-N_5$) synthesis and established the foundation for the synthesis of N_5^-ion.[4,5] In 2017, a system of ferrous bisglycinate and 3-chloroperbenzoic acid to oxidize and cut the C−N bond in $Ar-N_5$ to fabricate solid compounds containing $N_5^-$was reported.[6] This is the first time that a component of environmentally stable $(N_5)_6(H_3O)_3(NH_4)_4Cl$ which contains N_5^-anions has been separated. Very recently, a large amount of metal pentazolate salts including $[Na(H_2O)(N_5)]\cdot 2H_2O$ were synthesized via metal cation trapping of cyclo-N_5 anion.[7−11] However, the metal pentazolate salts cannot be directly used in secondary explosive due to limited energy. Therefore, nonmetallic pentazolate salts have become the direction of the subsequent discovery of pentazolate salt. Hu's group synthesized a series of nonmetallic pentazolate salts including $(NH_4)^+N_5^-$, $(N_2H_5)^+N_5^-$, $[N(CH_3)_4]^+N_5^-$, $(NH_3OH)^+N_5^-$, $[C(NH_2)_3]^+N_5^-$ using $[Mg(H_2O)_6]^{2+}$-$[(N_5)_2^-(H_2O)_4]^{2-}$ as raw material.[12] Soon after, Lu's group utilized the metathesis reaction of cationic hydrochloride and AgN_5 to obtain some nonmetallic pentazolate salts more conveniently like 3,4-diamino-1,2,4-triazolium, 3,6,7-triamino-7*H*-[1,2,4]triazolo[4,3-*b*][1,2,4]triazol-2-ium and so on.[13−16] However, the synthesized nonmetallic pentazolate salts show relatively low decomposition temperature (80.8−107.2 °C) and low crystals density (1.245−1.660 $g \cdot cm^{-3}$) (Scheme 1). The decomposition temperature of biguanidinium pentazolate reaches 124.8 °C, but the density is only 1.524 $g \cdot cm^{-3}$(150 K). Oppositely, oxalohydrazinium pentazolate has a relatively high density of 1.681 $g \cdot cm^{-3}$ (173 K), but the low decomposition temperature of 95 °C.

The molecular structure of furazan compounds contains many C−N, C=N, and N=N bonds, and has a high enthalpy of formation.[17] The coplanarity of furazan makes it denser, which is a key factor to improve detonation performance. Due to its heterocyclic system, furazan can form benzene-like structure to further increase its stability.[18,19]

Received: November 19, 2020
Revised: March 30, 2021
Published: April 12, 2021

https://doi.org/10.1021/acs.cgd.0c01574
Cryst. Growth Des. 2021, 21, 2690−2698

Scheme 1. Comparison of Three Novel Pentazolate Salts and Other Reported Pentazolate Salts

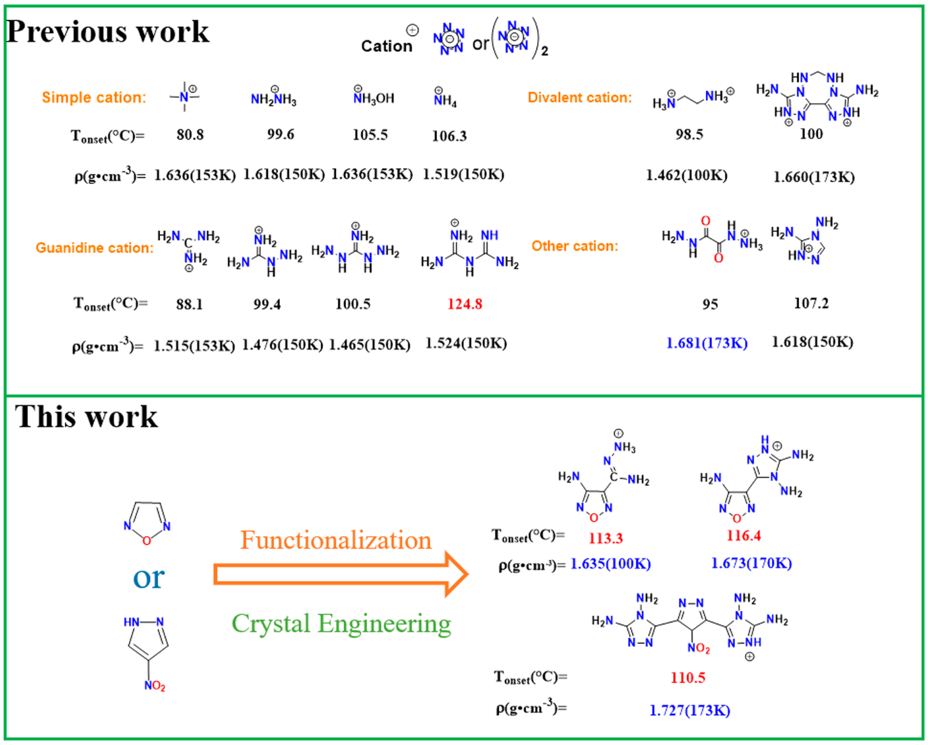

Therefore, the decomposition temperature of the synthetic derivatives of the furazan generally has good thermal stability. The 4-nitropyrazole demonstrates that three chain carbon atoms in pyrazole ring could enhance the impact insensitivity and give the backbone an opportunity for further functionalizations.[20,21] In addition to forming high-energy salts, introducing high-energy groups, and building high-energy metal−organic frameworks, the crystal engineering is also an effective method to improve the performance of new high-energy-density materials. Five types of $\pi-\pi$ stacking including face-to-face, wavelike, mixing, crossing and 3D-cube as energetic molecules have been reported (Figure 2).[22] Among these, the face-to-face, wavelike and 3D-cube crystal stacking can convert kinetic energy into layer sliding to absorb mechanical stimuli, which can improve stability and performance of compounds. Here, we reported the synthesis of three nonmetallic pentazole salt based on furazan or 4-nitropyrazole containing 4-amino-1,2,5-oxadiazole-3-carbohydrazonamide pentazolate (**6**), 5-(4-amino-1,2,5-oxadiazol-3-yl)-4*H*-1,2,4-triazole-3,4-diamine pentazolate (**7**), and 5,5′-(4-nitro-1*H*-pyrazole-3,5-diyl)-bis(4*H*-1,2,4-triazole-3,4-diamine) pentazolate (**8**). We achieved the planarization of molecular structures to increase their stability and density, in which compound **8** has the highest crystal density (1.722 g·cm^{-3}/173 K) of nonmetallic pentazole salts to date because of its face-to-face crystal stacking. Moreover, the quantum-chemical calculations were used to better comprehend the relationship of structure-properties.

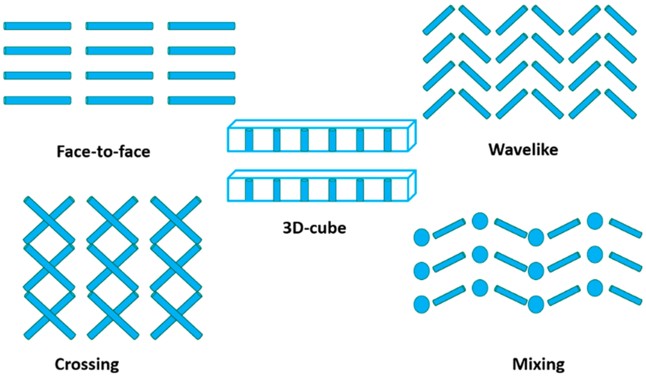

Figure 2. Five types of crystal packing.

RESULTS AND DISCUSSION

Synthesis. The synthetic pathway for all compounds is shown in Scheme 2. First, we added magnesium nitrate to an aqueous solution of $(N_5)_6(H_3O)_3(NH_4)_4Cl$ for trapping cyclo-N_5^- to form the stable compound $[Mg(H_2O)_6]^{2+}$-$[(N_5)_2^-(H_2O)_4]^{2-}$. After that, AgN_5 was obtained by the reaction of $[Mg(H_2O)_6]^{2+}[(N_5)_2^-(H_2O)_4]^{2-}$ with $AgNO_3$ in $MeOH/H_2O$. Amidrazones and 4,5-diaminotriazole groups were generally introduced into molecular structure to be further converted into cationic hydrochlorides. Among them, amidrazone group can be obtained by the reaction of cyano group and hydrazine hydrate. 4-amino-1,2,5-oxadiazole-3-carbohydrazonamide (**2**) was synthesized from 3-amino-4-cyanofurazan (**1**) and hydrazine hydrate at room temperature in 2-propanol with 73.93% yield.[23] With the cyclization reaction of carboxyl and diaminoguanidine hydrochloride, 3-amino-4-carboxylic acid furazan can react with 1,3-diaminoguanidine hydrochloride to form 3-amino-4-(4,5-diamino-1,2,4-triazole-3-yl)furazan (**3**) according to literature.[24] Similarly, 3,5-dicarboxylic acid-4-nitropyrazole and 1,3-diaminoguanidine hydrochloride are reacted in the presence of P_2O_5/H_3PO_4 system for cyclization to obtain compound **5** with 86.2% yield. Finally, 4-amino-1,2,5-oxadiazole-3-carbohydrazonamide pentazolate (**6**), 3-amino-4-(4,5-diamino-1,2,4-tria-

Scheme 2. Synthesis of Pentazole Nonmetallic Salts 6−8

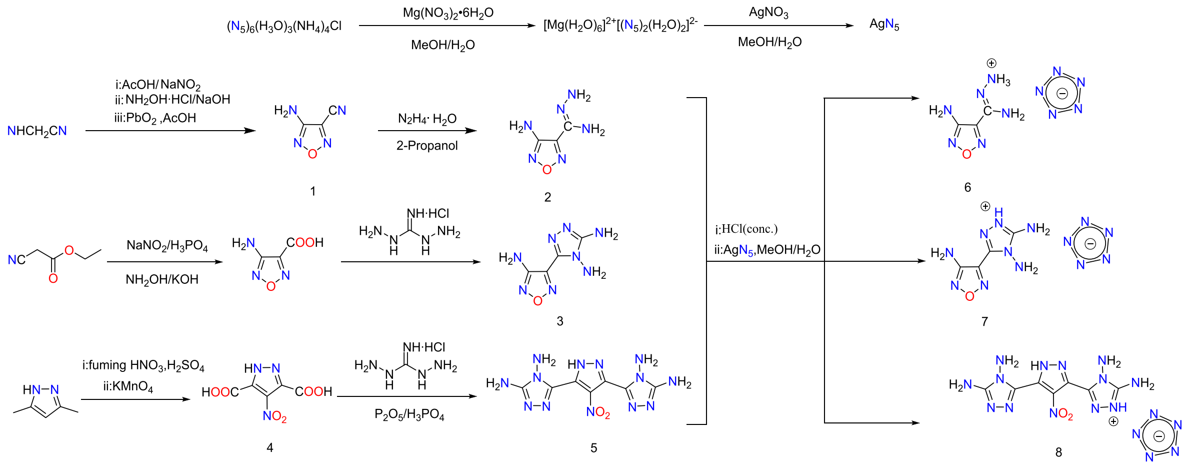

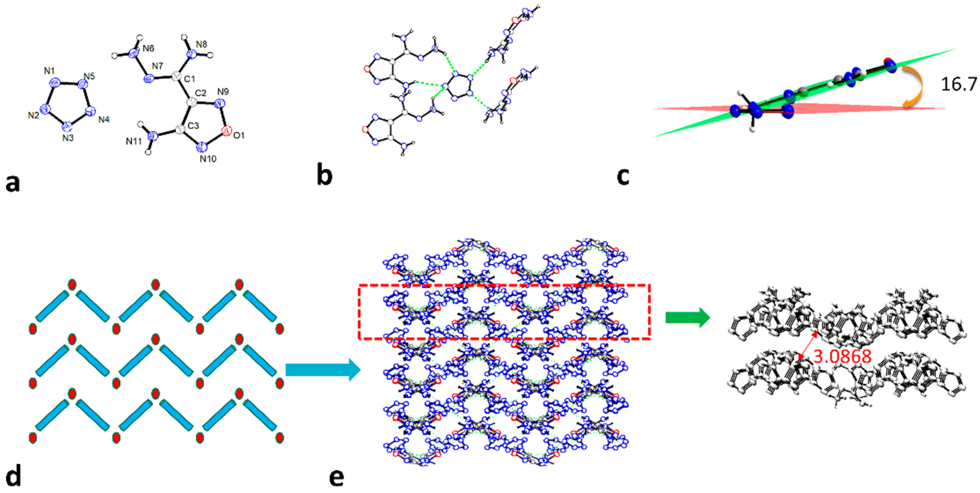

Figure 3. (a) Molecular structure of compound **6**. Thermal ellipsoids are drawn at the 50% probability level. (b) Supramolecular interaction between N_5^- and the nearby cation. (c) Molecular planarity of compound **6**. (d) Schematic diagram of crystal packing of **6**. Lines represent cations, and the ellipsoid indicates N_5^-. (e) Packing diagram of **6**. Green lines represent strong hydrogen bonding.

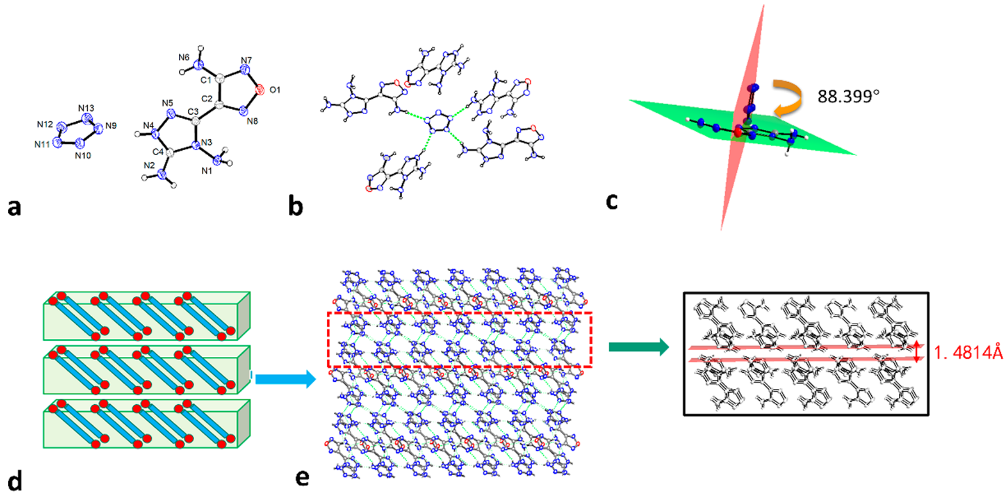

Figure 4. (a) Molecular structure of compound 7. Thermal ellipsoids are drawn at the 50% probability level. (b) Supramolecular interaction between N_5^- and the nearby cation. (c) Molecular planarity of compound 7. (d) Schematic diagram of crystal packing of **8**. Lines represent cations, and the ellipsoid indicates N_5^-. (e) Packing diagram of 7. Green lines represent strong hydrogen bonding.

zole-3-yl)-furazan pentazolate (7), and 4- nitro-3,5-bis(3,4-diamino-1,2,4-triazol-5-yl)-1*H*-pyrazole pentazolate (8) was synthesized via metathesis reactions of AgN_5 with the respective cationic hydrochloride in $MeOH/H_2O$ at 25 °C

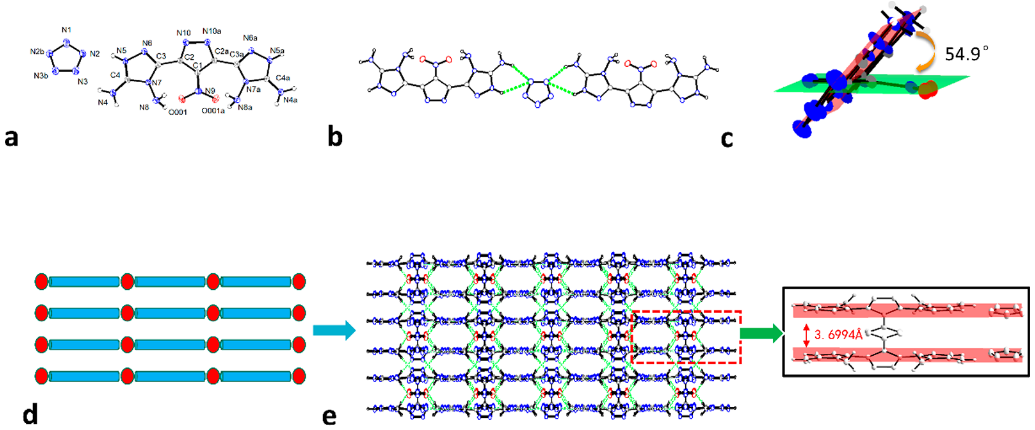

Figure 5. (a) Molecular structure of compound **8**. Thermal ellipsoids are drawn at the 50% probability level. (b) Supramolecular interaction between N_5^- and the nearby cation. (c) Molecular planarity of compound **8**. (d) Schematic diagram of crystal packing of **8**. Lines represent cations, and the ellipsoid indicates N_5^-. (e) Packing diagram of **8**. Green lines represent strong hydrogen bonding.

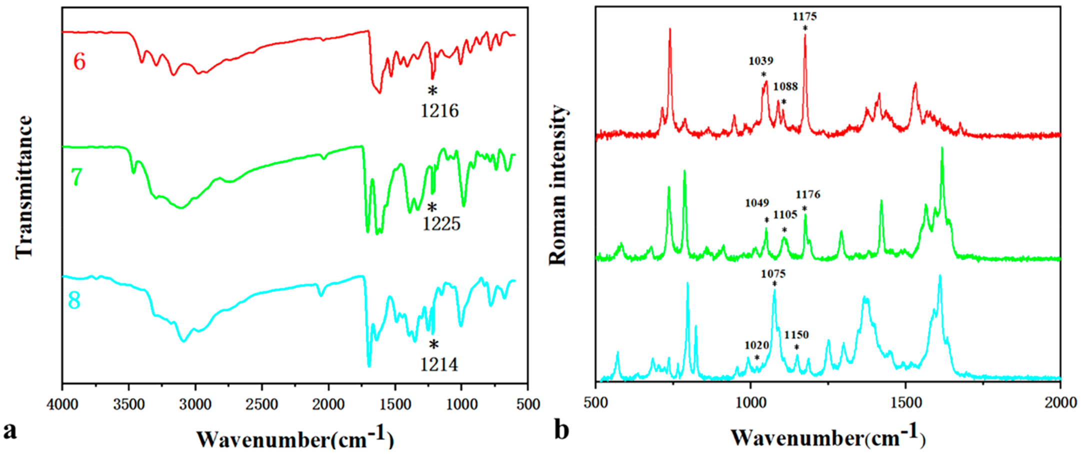

Figure 6. (a) IR spectra of **6**−**8**. (b) Raman spectra of **6**−**8**.

for 8 h. Notably, the entire reaction process needs to be carried out in a dark environment owing to the sensitivity of AgN_5 to light.

Single-Crystal X-ray Analysis. Suitable single-crystals of **6**, **7**, and **8** were obtained by slow evaporation of methanol at 25 °C. The structures of these salts are shown in Figure 3−5, and their crystallographic data are given in the Table S1.

Compound **6** crystallizes in the monoclinic space group $P2_1/c$ with four molecules in the lattice units (Z = 4) and a calculated density of 1.635 g·cm^{-3} at 100 K. The average bond length of each N_5^- anion is 1.3218 Å, longer than that of most reported metallic pentazole salts (1.314−1.320 Å).[7,8,11] The C−N bond length of C-amino groups (C1−N8, 1.3345(29) Å) are almost equal to that of the furazan rings (C3−N11:1.3394(32) Å). All carbon and nitrogen atoms of cations are in the same plane supported by the twist angle (N6−N7−C1−C2: − 178.908(168)°; N8−C1−C2−C3:175.641(106)°; N9−C2−C1−N8:3.346(300)°). As shown in Figure 3(b), four hydrogen bonds from four cations are used to stabilize one cylco-N_5^- anion (N8−H8A···N1:2.054(241) Å; N6−H6C··· N2:2.034(21) Å; N6−H6A···N4:2.378(21) Å;N11−H11B··· N4:2.484(259) Å; N6−H6C···N5:2.038(20) Å). Except hydrogen bonds between cyclo-$N_5^-$and cations, there is a strong intramolecular hydrogen bonds(N11−H11B··· N7:2.294(237) Å) in each cation. The dihedral angle between cation (plane through O1, C2 and C3) and N_5^- anion (plane through N1, N2 and N5) are 16.707(407)° in Figure 3(c), indicating that they are basically coplanar. In Figure 3d and 3e, **6** presents a wavelike crystal packing with a layer spacing of 3.0868 Å. The cyclo- N_5^- anions act as the apex of the wave, which can be interpreted by cyclo-N_5^- anions acting as hydrogen bond mediation to some extent. These hydrogen bonds are attributed to the low sensitivity of **6**.[22]

Compound **7** crystallizes in the $P2/c$ space group with four molecules per unit cell, and has a calculated density of 1.673 g·cm^{-3} (170 K). Each N_5^- anion is surrounded by four cations to form hydrogen bonds (N2−H2A··· N11:2.030 Å; N2−H2B··· N10:2.130 Å; N4−H4··· N9:2.010 Å; N6−H6A··· N13:2.2400 Å) (Figure 4b), and four strong intra hydrogen bonds(N1−H1A···N7:2.428(18) Å; N2−H2B···N1:2.5600 Å; N6−H6B···N5:2.4000 Å; N6- H6B···O1:2.2800 Å) in the molecule. The torsion angle of the cation reveals an almost coplanar ring (N1−N3−C3−C2:1.833(233)°,C2−C3−N5−N4:175.800(258)°,C1−C2−C3−N3:176.608(136)°,N8−C2−C3−N5,173.407(140)°), but the furazan ring and N_5^- ring of **7** are noncoplanar, which is clearly evident from the dihedral angle of the furazan ring and N_5^- ring (88.399)°) intuitively (Figure 4c). This almost vertical crystal structure forms a special kind of crystal packing. As shown in Figure 4d and 4e, two adjacent N_5^- anions served as the connection point and cations acted as pillars of the network. Then, the layers with a layer spacing of 1.4814 Å stack into a stratiform structure to form the 3D-cube packing system. Meanwhile, large amount hydrogen bonds existing between layers or in the network could enhances the strength of crystal packing as well as the stability of compound.

Here, each proton in the cation of compound **8** (N5 and N5a) has a 50% occupancy due to its symmetry, indicating **8** is univalent. Compound **8** crystallizes in the $C2/m$ space group with four molecules per unit cell. The density of **8** is 1.722 g·cm^{-3} at 173 K which is the highest density nonmetallic pentazole salts reported so far. All N−N bond length of cyclo-N_5^- of **8** are 1.3158(32), 1.3158(32), 1.3265(64), 1.3265(64), 1.3093(39) Å forming a symmetrical structure. The average bond length is 1.3188 Å lower thancompound **6**. Each N_5^- anion is surrounded by two cations to form hydrogen bonds with it (N4−H4A···N3:2.1 Å, N5−H5··· N3:2.6 Å) (Figure 5b). Each triazole ring (plane through N5, N6 and N7 or N5a, N6a and N7a) is basically coplanar (5.591(171)°) with the N_5^- anion ring. In Figure 5c, since the nitro group (N9) on the pyrazole ring is affected by the steric hindrance of the amino group (N8 and N8a) on the triazole ring, the pyrazole ring(plane through C1,N10 and N10a) is deflected with 54.9° of the dihedral angle with triazole (plane through N5,N6 and N7). As can be seen from Figure 5d and 5e, **8** is layer-by-layer stacking with 3.6994 Å of the interlayer distance. This crystal packing may be attributed to its high density and low sensitivity.

Vibrational Spectroscopy. Infrared (IR) and Raman (RA) spectra (785 nm excitation) of compounds **6**−**8** were identified to provide valuable insight into the vibrational intra- and inter- molecular bonds. In the IR spectra (Figure 6a), the cyclo-N_5^- anion of **6**−**8** exhibits a sharp peak at 1215−1225 cm^{-1} which is consistent with the result of $(N_5)_6(H_3O)_3(NH_4)_4Cl$.[6] Furthermore, when compared to compound **7**, the IR spectra of **6** and **8** shows that the peaks of the cyclo-N_5^- anion are red-shifted by about 10 cm^{-1}, which maybe result from the fact that crystal packings of **6** and **8** exhibit stronger N−H···π interactions than that of compound **7**. According to group theory,[12] the planar cyclo-N_5^- anion's stretching modes span A1′ + E1′ + 2E2′ + E2′ in the context of D_{5h} symmetry. As can be seen from RA spectra (Figure 6b), three characteristic peaks of cyclo-N_5^- of **6**−**8** are observed in the range of 1150−1176 cm^{-1} (A1′), 1088−1105 cm^{-1} (E2′), and 1020−1049 cm^{-1} (E2′), in basically agreement with the result of $(N_5)_6(H_3O)_3(NH_4)_4Cl$.[6] The discrepancies among three compounds can result from the strong intermolecular forces between cations and cyclo-N_5^- anion.

Thermal Stability. The thermal stability of compounds **6-8** was analyzed via differential scanning calorimetry (DSC) scanning with a heating rate of 5 °C min $^{-1}$ over the temperature range from 30 to 450 °C. As shown in Figure 7, salts **6**, **7**, and **8** all decomposed (**6**:113.3 °C; **7**:116.4 °C; **8**:110.5 °C) without melting and step by step in the range of 100−350 °C. They all exhibit thermal stabilities beyond 110 °C (onset), higher than that of other pentazolate salts (Figure 7). The exothermic peak of **6** is observed an obvious endothermic peak at 244 °C which should be the melting of cationic azide produced by the decomposition of pentazolate salts.[6,13] Correspondingly, compound **8** immediately has an endothermic peak which could be the volatilization of hydragoic acid (HN_3) after the decomposition of the pentazolate anion.[12] Therefore, the cation also has a certain degree of influence on the decomposition products (HN_3 or organic azide salt) of pentazolate. To better demonstrate the effect of furazan and 4-nitropyrazole on the decomposition temperature of pentazolate salt, 11 reported pentazolate salts are selected for comparison.[12,13,15,16]

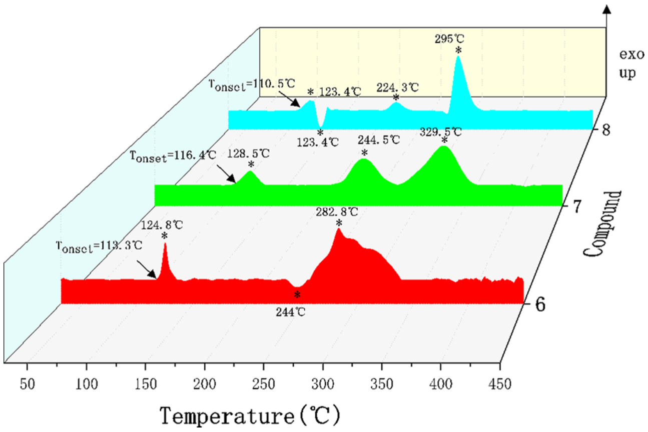

Figure 7. DSC curves of **6**, **7**, and **8**.

As shown in Figure 8, all pentazolate salts are arranged from low to high value by decomposition temperature (red pillar), and the calculated density (blue pillar) at 273 K is used as the density change. It can be clearly seen that decomposition temperature of **6**, **7**, and **8** are higher than that of $N(CH_3)_4^+N_5^-$ by nearly 30 °C about 38% increase and also better than that of simple, guanidines and azole pentazlate salts. Synchronously, the crystal density is also maintained at a high level (1.615−1.695 g·cm^{-3}) which is more superior to most reported other pentazolate salts (1.126−1.601 g·cm^{-3}). Overall, furazan and 4-nitropyrazole skeleton have a good promotion effect on the decomposition temperature and density of pentazolate salt.

To furthermore understand the relationship of structure-properties, two-dimensional (2D) fingerprints and Hirshfeld surface were used to analyze the weak interactions and hydrogen bonds of pentazolate salts.[25] The sensitivity of **6-8** can be described by the shape of Hirshfeld surfaces, and the regions of red or blue on which represent high or low close contact populations.[26,27]

From Figure 9c,i, due to the coplanarity of **6** and **8**'s anion and cation, most of the red dots (intermolecular interaction) are located at the edge of the surface. Therefore, the molecular plane can be stacked as much as possible to resist external stimuli in this way, which results in its low sensitivity and good stability. In Figure 9a,d,g, the sharp peaks on bottom left (H−O and O−H, H−N and N−H interactions) of 6, 7, and 8 represent hydrogen bonds between surrounding molecules.[28] Owing to the introduction of oxygen atoms, the numerous hydrogen-bonding interactions (H−O and O−H, N−H and H−N, 63% for 6, 55% for 7, and 56% for 8) partly contribute to be insensitive between molecules. Correspondingly, low sensitivity is also partly attribute to π−π stacking interactions (N−C and C−N, O−N and N−O interactions, 13% for 6, 11% for 7, 13% for 8) between layer and layer of molecular.

To further research the interactions among crystals **6**, **7**, and **8**, the noncovalent interaction (NCI) analysis (Figure 10) of **6**, **7**, and **8** calculated by Multiwfn[29,30] were used on the basis of electron density.[31] For the color-filled reduced density gradient (RDG) iso-surface of the NCI plots, the stronger attractions are represented by blue surfaces and the π−π interactions are expressed by large green iso-surfaces. From Figure 10, the π−π interactions exist in abundance in **6**, **7**, and **8**. Meanwhile,

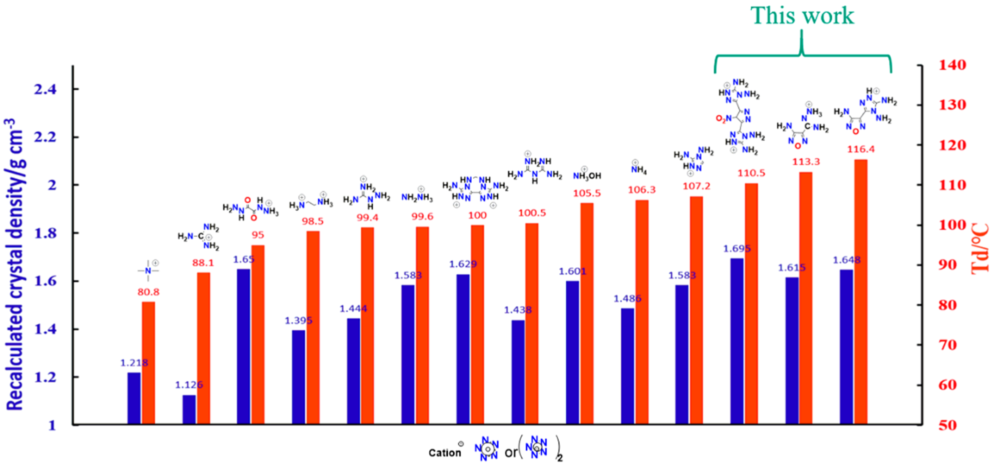

Figure 8. Decomposition temperature and recalculated crystal density (273 K) of compound **6**, **7**, and **8** and other reported pentazolate salts.

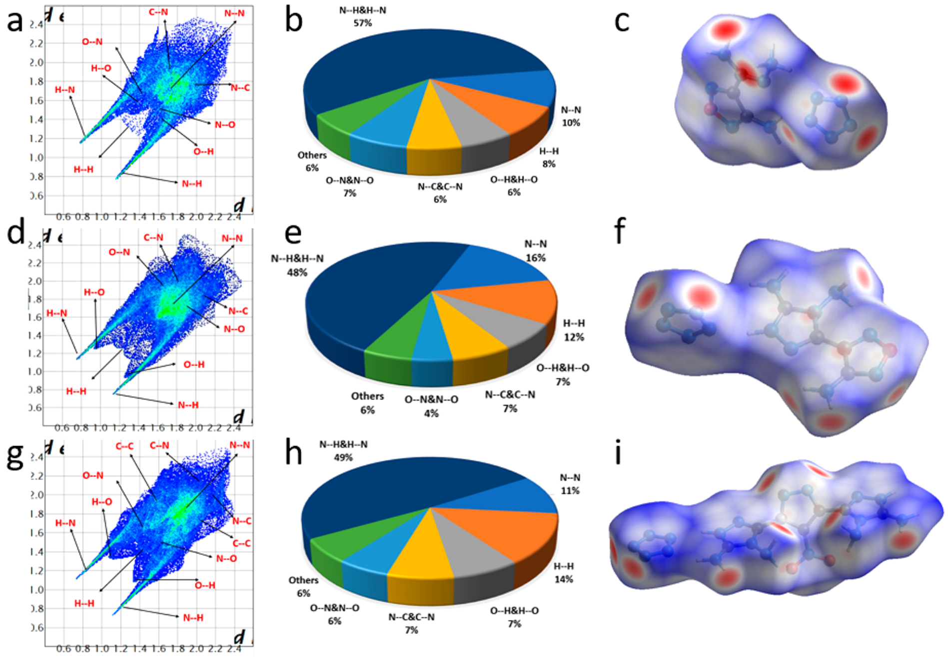

Figure 9. 2D fingerprint plots, Hirshfeld surfaces, and individual atomic contacts percentage of the Hirshfeld surface for **6** (a)−(c), **7** (d)−(f), and **8** (g)−(i).

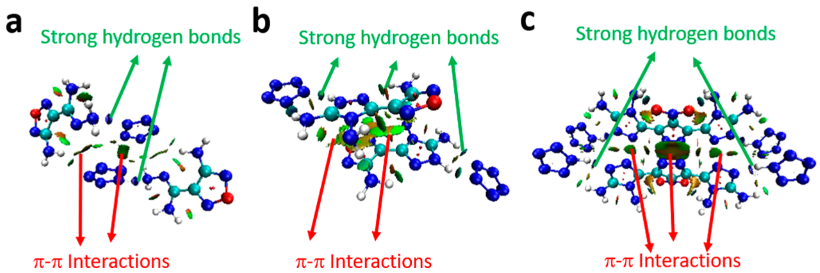

Figure 10. (a)−(c) Noncovalent interactions analysis of gradient iso-surfaces (blue, strong attraction; green, $\pi-\pi$ interactions; red, strong repulsion) for **6** (a), **7** (b), and **8** (c)

intramolecular hydrogen bonds denoted by blue, ellipse, and shaped surfaces theoretically were accumulations of electron density. The face-to-face $\pi-\pi$ interactions are widely distributed among parallel cyclo-N_5^- rings and between a cyclo-N_5^- ring and a cationic ring. These could be in favor of the desensitization of compounds. As salt **8** stacked layer-by-layer and was tightly packed (short interlayer distance), $\pi-\pi$ interactions are very strong (Figure 10c), which may lead to its high density and low sensitivity.

Physic and Energetic Properties. The heat of formation of the cyclo-N_5^- anion has been calculated in the literature.[13]

Table 1. Physicochemical Properties of 6−8 Compared with Other Pentazolate Salts

compound	T_d[a] [°C]	ρ[b] [g·cm^{-3}]	ΔH_f[c] [(kJ·mol^{-1})/(kJ·g^{-1})]	D[d] [m·s^{-1}]	P[e] [GPa]	IS[f] [J]	FS[g] [N]	OB[h] %
6	113.3	1.615/1.635(100 K)	789.0/3.7	8594	26.4	>40	>360	−41.27
7	116.4	1.648/1.673(170 K)	985.7/3.89	8700	27.8	36	>360	−41.07
8	110.5	1.695/1.722(173 K)	1084.2/2.86	8124	23.7	>40	>360	−42.29
$N(CH_3)_4{}^+N_5{}^-$ [i]	80.8	1.218/1.245(153 K)	635.8/4.42	7906	17.9	35	>360	−111.1
$C(NH_2)_3{}^+N_5{}^-$ [i]	88.1	1.483/1.515(153 K)	312.3/2.40	7078	15.7	24	>360	−49.2
$AG^+N_5{}^-$ [j]	99.4	1.444/1.476(150 K)	392.1/0.58	7986	20.6	>40	>360	−49.7
$DABTT_2{}^+(N_5{}^-)_2$ [j]	100	1.629/1.660(173 K)	1341.2/3.83	7825	24.5	10	120	−45.7
DAG^+N_5 [j]	100.5	1.438/1.465(150 K)	508.0/3.15	8001	22.3	25	240	−50
$DAT^+N_5{}^-$ [j]	107.2	1.583/1.618(150 K)	639.7/4.17	7965	24.9	>40	>360	−47.06
$BG^+N_5{}^-$ [j]	124.8	1.491/1.524(150 K)	1362.0/7.91	9450	34.3	35	300	−55.8
RDX	204	1.806	80.0/0.36	8872	34.7	7.4	120	0
HMX	279	1.90	104.8/0.36	9254	39.2	7	120	0

[a] Decomposition temperature. [b] Density, recalculated using a gas pycnometer at 25°/crystal densities. [c] Calculated solid heat of formation by the Guassian 09. [d] Calculated detonation velocity (EXPLO5 Version 6.05). [e] Calculated detonation pressure (EXPLO5 Version 6.05). [f] Impact sensitivity. [g] Friction sensitivity. [h] Oxygen balance (based on CO) for $C_aH_bO_cN_d$, 1600(c-a-b/2)/Mw. [i] From ref 12. [j] From ref 13. AG^+: aminoguanidinium. $DABTT^{2+}$: 3,9-diamino-6,7-dihydro-5*H*-bis([1,2,4]triazolo)[4,3-*e*:3′,4′-*g*][1,2,4,5]tetrazepine-2,10-diium. DAG: diaminoguanidinium. DAT^+: 3,4-diamino-1,2,4-triazolium. BG: biguanidinium.

And that of other cations were calculated by the Gaussian 09 program.

As summarized in Table 1, the enthalpy of formation and detonation formation between three newly synthesized pentazolate salts and other reported salts are listed. Due to the introduction of furazan and 4-nitropyrazole, salts **6**−**8** exhibited positive heats of formation (789−1084.2 kJ·mol^{-1}), which exceeded that of most others salts (312.3−639.7 kJ·mol^{-1}) except $DABTT_2{}^+(N_5{}^-)_2$ (1341.2 kJ·mol^{-1})[16] and $BG^+N_5{}^-$ (1362.0 kJ·mol^{-1}).[13] Meanwhile, the detonation performance of those salts was calculated using the EXPLO5 (Version 6.05) program via HOF and measured density.[32] The detonation velocity shown in Table 1 for **6**−**8** are in the range 8124−8700 m·s^{-1}, of which **8** is similar to RDX but lower than HMX. By contrast with different energetic cations, the detonation performances of **6** and **7** are superior to that of $N(CH_3)_4{}^+N_5{}^-$ (7906 m·s^{-1}),[12] $C(NH_2)_3{}^+N_5{}^-$ (7078 m·s^{-1}),[12] $AG^+N_5{}^-$ (7986 m·s^{-1}),[13] $DABTT^{2+}(N_5{}^-)_2$ (7825 m·s^{-1}),[16] and $DAG^+N_5{}^-$ (8001 m·s^{-1}),[13] indicating that furazan and 4-nitropyrazole as energetic cations could contribute to improving the performance of pentazolate salts.

Usually, the contradiction between energetic property and safety hinders the application of HEDM materials. Therefore, the sensitivity tests (impact and friction sensitivity) of **6**−**8** were carried out by standard BAM techniques.[33] For**6** and **8**, they have pretty low sensitivity (IS > 40 J, FS > 360 N) and are more insensitive than RDX (IS = 7.4 J, FS = 120 N) and HMX (IS = 7, FS = 120 N), which arises from the influence of stable wavelike and layer-by-layer stacking. Even though **7** presents a crossing crystal packing, it also exhibits better insensitive properties than other pentazolate salts (Table 1) due to its two insensitive groups, including a furazan ring and triazole, implying that the sensitivity mechanism relying on a single factor is not enough. In general, salts **6**−**8** show higher density, better thermal stability, acceptable detonation performance, and lower sensitivity compared with most other pentazolate salts.

The most vital parameter for determining the performance of a composite propellant is specific impulse (I_{sp}), which is mainly determined by the combustion temperature and the average molecular mass of combustion gas during the combustion process.[34] A high specific impulse propellant has an advantage due to its more thrust generated. The specific impulse value of the glycidyl azide polymer (GAP) based propellant formula[35,36] including 10 wt % GAP, 5 wt % aluminum, 60 wt % AP, and 25 wt % RDX was determined by the EXPLO5 (v6.05) program. As we can see in Table 2, with replacement of RDX by three target compounds, compositions A (salt **6** instead of RDX) and B (salt **7** instead of RDX) exhibit specific impulse values (A, I_{sp} = 262.1 s; B, I_{sp} = 263.9 s) higher than that of composition D (I_{sp} = 261.8 s). Due to relatively low detonation properties, the specific impulse (I_{sp}) of composition C (salt **8** instead of RDX) is 259.0 s, very close to that of composition D. Therefore, these three compounds have great promise in the solid propulsion formulations.

Table 2. Propellant Performances

composition	GAP[a] (%)	Al[b] (%)	AP[c] (%)	compound (%)	I_{sp}[d] (s)
A	10	5	60	25 (salt **6**)	262.1
B	10	5	60	25 (salt **7**)	263.9
C	10	5	60	25 (salt **8**)	259.0
D	10	5	60	25 (RDX)	261.8

[a] Glycidyl azide polymer. [b] Aluminum. [c] Ammonium perchlorate. [d] Specific impulse under isobaric conditions at 7 MPa.

CONCLUSIONS

In summary, on the basis of the characteristics of high stability, coplanarity, and good performance of furazan and 4-nitropyrazole, three novel pentazole salts with stable crystal stacking have been synthesized. These three salts exhibit good thermal stability (**6**, 113.3 °C; **7**, 116.4 °C; **8**, 110.5 °C), relatively high density (1.635−1.722 g·cm^{-3}), low sensitivity (IS > 35 J, FS > 360 N), and acceptable detonation property (8124−8700 m·s^{-1}). Moreover, with a supplement of salt **6** or **7**, the glycidyl azide polymer (GAP) based propellant formula (10 wt % GAP, 5 wt % aluminum, 60 wt % AP) shows high specific impulse (**6**, I_{sp} = 262.1 s; **7**, I_{sp} = 263.9 s). For practical applications, this work provides a new perspective of crystal engineering to further increase the stability and density of the nonmetallic pentazole salts.

ASSOCIATED CONTENT

Supporting Information

The Supporting Information is available free of charge at https://pubs.acs.org/doi/10.1021/acs.cgd.0c01574.

Experimental section, computational details, crystallographic data for target compounds, and spectra (PDF)

Accession Codes

CCDC 2015456, 2015523, and 2015527 contain the supplementary crystallographic data for this paper. These data can be obtained free of charge via www.ccdc.cam.ac.uk/data_request/cif, or by emailing data_request@ccdc.cam.ac.uk, or by contacting The Cambridge Crystallographic Data Centre, 12 Union Road, Cambridge CB2 1EZ, UK; fax: +44 1223 336033.

AUTHOR INFORMATION

Corresponding Authors

Bingcheng Hu − *School of Chemical Engineering, Nanjing University of Science and Technology, Nanjing, Jiangsu 210094, China*; orcid.org/0000-0002-0371-8128; Email: hubc@njust.edu.cn

Guangbin Cheng − *School of Chemical Engineering, Nanjing University of Science and Technology, Nanjing, Jiangsu 210094, China*; orcid.org/0000-0003-0501-6469; Email: gcheng@mail.njust.edu.cn

Authors

Wei Hu − *School of Chemical Engineering, Nanjing University of Science and Technology, Nanjing, Jiangsu 210094, China*

Hongwei Yang − *School of Chemical Engineering, Nanjing University of Science and Technology, Nanjing, Jiangsu 210094, China*; orcid.org/0000-0003-4763-2972

Jieyi Chen − *School of Chemical Engineering, Nanjing University of Science and Technology, Nanjing, Jiangsu 210094, China*

Chong Zhang − *School of Chemical Engineering, Nanjing University of Science and Technology, Nanjing, Jiangsu 210094, China*

Chengguo Sun − *School of Chemical Engineering, Nanjing University of Science and Technology, Nanjing, Jiangsu 210094, China*; orcid.org/0000-0003-3580-2153

Complete contact information is available at: https://pubs.acs.org/10.1021/acs.cgd.0c01574

Notes

The authors declare no competing financial interest.

ACKNOWLEDGMENTS

The financials of the National Natural Science Foundation of China (Nos. 21875110, 21975128, 11972178, and 21903044) and the Science Challenge Project (TZ2018004) support this work.

REFERENCES

(1) Zhang, W.; Zhang, J.; Deng, M.; Qi, X.; Nie, F.; Zhang, Q. A Promising High-energy-density Material. *Nat. Commun.* **2017**, *8*, 181.

(2) Christe, K. O. Recent Advances in The Chemistry of N_5^+, N_5^- And High-oxygen Compounds. *Propellants, Explos., Pyrotech.* **2007**, *32*, 194−204.

(3) Christe, K. O. Polynitrogen Chemistry Enters the Ring. *Science* **2017**, *355*, 351−351.

(4) Huisgen, R.; Ugi, I. Solution of A Classical Problem of Organic Nitrogen Chemistry. *Angew. Chem.* **1956**, *68*, 705−706.

(5) Huisgen, R.; Ugi, I. Die Lösung Eines Klassischen Problems Der Organischen Stickstoffchemie. *Chem. Ber.* **1957**, *90*, 2914−2927.

(6) Zhang, C.; Sun, C.; Hu, B.; Yu, C.; Lu, M. Synthesis and Characterization of The Pentazolate Anion Cyclo-N_5^- In $(N_5)_6(H_3O)_3(NH_4)_4Cl$. *Science* **2017**, *355*, 374−376.

(7) Xu, Y.; Wang, Q.; Shen, C.; Lin, Q.; Wang, P.; Lu, M. A Series of Energetic Metal Pentazolate Hydrates. *Nature* **2017**, *549*, 78−81.

(8) Xu, Y.; Wang, P.; Lin, Q.; Lu, M. A Carbon-Free Inorganic-Metal Complex Consisting of An All-Nitrogen Pentazole Anion, A Zn (II) Cation and H_2O. *Dalton Trans.* **2017**, *46*, 14088−14093.

(9) Zhang, C.; Yang, C.; Hu, B.; Yu, C.; Zheng, Z.; Sun, C. A Symmetric $Co(N_5)_2(H_2O)_4 \bullet 4H_2O$ High-Nitrogen Compound Formed by Cobalt (II) Cation Trapping of A Cyclo-N_5^- Anion. *Angew. Chem., Int. Ed.* **2017**, *56*, 4512−4514.

(10) Xu, Y.; Wang, P.; Lin, Q.; Mei, X.; Lu, M. Self-Assembled Energetic 3D Metal-Organic Framework $[Na_8(N_5)_8(H_2O)_3]_n$ Based On Cyclo-N_5^-. *Dalton Trans.* **2018**, *47*, 1398−1401.

(11) Wang, P.; Xu, Y.; Wang, Q.; Shao, Y.; Lin, Q.; Lu, M. Self-Assembled Energetic Coordination Polymers Based on Multidentate Pentazole Cyclo-N_5^-. *Sci. China Mater.* **2019**, *62*, 122−129.

(12) Yang, C.; Zhang, C.; Zheng, Z.; Jiang, C.; Luo, J.; Du, Y.; Sun, C.; Hu, B.; Christe, K. O. Synthesis and Characterization of Cyclo-Pentazolate Salts of NH_4^+, NH_3OH^+, $N_2H_5^+$, $C(NH_2)_3^+$, And $N(CH_3)_4^+$. *J. Am. Chem. Soc.* **2018**, *140*, 16488−16494.

(13) Xu, Y.; Tian, L.; Li, D.; Wang, P.; Lu, M. A Series of Energetic Cyclo-Pentazolate Salts: Rapid Synthesis, Characterization, And Promising Performance. *J. Mater. Chem. A* **2019**, *7*, 12468−12479.

(14) Xu, Y.; Lin, Q.; Wang, P.; Lu, M. Syntheses, Crystal Structures and Properties of A Series Of 3D Metal-Inorganic Frameworks Containing Pentazolate Anion. *Chem. - Asian J.* **2018**, *13*, 1669−1673.

(15) Xu, Y.; Lin, Q.; Wang, P.; Lu, M. Stabilization of The Pentazolate Anion in Three Anhydrous and Metal-Free Energetic Salts. *Chem. - Asian J.* **2018**, *13*, 924−928.

(16) Tian, L.; Xu, Y.; Lin, Q.; Wang, P.; Lu, M. Syntheses of Energetic Cyclo-Pentazolatesalts. *Chem. - Asian J.* **2019**, *14*, 877−882.

(17) Ivanova, O. A.; Averina, E. B.; Kuznetsova, T. S.; Zefirov, N. S. Synthesis of New 3,4-Disubstituted Furazans. *Chem. Heterocycl. Compd.* **2000**, *36*, 1091−1096.

(18) Alt, G. H.; Speziale, A. J. Reactions of Enamines. V. The Acylation of Enamino Ketones. *J. Org. Chem.* **1964**, *29*, 798−800.

(19) Talawar, M. B.; Sivabalan, R.; Senthilkumar, N.; Prabhu, G.; Asthana, S. N. Synthesis, Characterization and Thermal Studies on Furazan- And Tetrazine-Based High Energy Materials. *J. Hazard. Mater.* **2004**, *113*, 11−25.

(20) Zhang, J.; He, C.; Parrish, D. A.; Shreeve, J. M. Nitramines with Varying Sensitivities: Functionalized Dipyrazolyl-N-Nitromethanamines As Energetic Materials. *Chem. - Eur. J.* **2013**, *19*, 8929−8936.

(21) Zhang, J.; He, C.; Parrish, D. A.; Shreeve, J. M. 4-Chloro-3,5-Dinitropyrazole: A Precursor for Promising Insensitive Energetic Compounds. *J. Mater. Chem. A* **2013**, *1*, 2863−2868.

(22) Yin, P.; Mitchell, L. A.; Parrish, D. A.; Shreeve, J. M. Energetic N-Nitramino/N-Oxyl-Functionalized Pyrazoles with Versatile π-π Stacking: Structure-Property Relationships of High-Performance Energetic Materials. *Angew. Chem., Int. Ed.* **2016**, *55*, 14409−14411.

(23) Ding, Z.; Cao, W.; Huang, J.; et al. Synthesis, Structure Analysis And Thermal Behavior Of Two New Complexes: $Cu(NH_3)_4(AFT)_2$ And $Cu(C_3H_6N_2H_4)_2(AFT)_2$. *J. Mol. Struct.* **2019**, *1175*, 373−378.

(24) Liu, Y.; Xu, Y.; Sun, Q.; Lu, M. Energetic Furazan-Triazoles With High Thermal Stability And Low Sensitivity: Facile Synthesis, Crystal Structures And Energetic Properties. *CrystEngComm* **2019**, *21*, 6093−6099.

(25) Zhang, J.; Zhang, Q.; Vo, T. T.; Parrish, D. A.; Shreeve, J. M. Energetic Salts With Π-Stacking and Hydrogen-Bonding Interactions Lead the Way to Future Energetic Materials. *J. Am. Chem. Soc.* **2015**, *137*, 1697−1704.

(26) Spackman, M. A.; McKinnon, J. J. Fingerprinting Intermolecular Interactions in Molecular Crystals. *CrystEngComm* **2002**, *4*, 378−392.

(27) Spackman, M. A.; Jayatilaka, D. Hirshfeld Surface Analysis. *CrystEngComm* **2009**, *11*, 19−32.

(28) Lu, T.; Chen, F. Multiwfn: A Multifunctional Wavefunction Analyzer. *J. Comput. Chem.* **2012**, *33*, 580−592.

(29) Politzer, P.; Murray, J. S. Some Molecular/Crystalline Factors That Affect the Sensitivities of Energetic Materials: Molecular Surface Electrostatic Potentials, Lattice Free Space and Maximum Heat of Detonation Per Unit Volume. *J. Mol. Model.* **2015**, *21*, 25.

(30) Johnson, E. R.; Keinan, S.; Sanchez, P. M.; Garcıa, J. C.; Cohen, A. J.; Yang, W. Revealing Noncovalent Interactions. *J. Am. Chem. Soc.* **2010**, *132*, 6498−6506.

(31) Suceska, M. Calculation of The Detonation Properties Of C-H-N-O Explosives. *Propellants, Explos., Pyrotech.* **1991**, *16*, 197−202.

(32) Suceska, M. *EXPLO5 Program*; Brodarski Institute: Zagreb, Croatia, 2011.

(33) *Tests were conducted according to the UN Recommendations on the Transport of Dangerous Goods, Manual of Tests and Criteria*, 5th rev. ed.; United Nations Publication: New York, 2009.

(34) Klapötke, T. M. *Chemistry of high-energy materials*, 2nd ed.; De Gruyter: Berlin, 2012.

(35) Klapötke, T. M.; Krumm, B.; Reith, T. Polyfunctional Energetic Nitrates Derived From Tris(Hydroxymethyl)Aminomethane (Tris). *Eur. J. Org. Chem.* **2017**, *2017*, 3666−3673.

(36) Song, S.; Wang, Y.; He, W.; Wang, K.; Yan, M.; Yan, Q.; Zhang, Q. Melamine N-Oxide Based Self-Assembled Energetic Materials with Balanced Energy & Sensitivity And Enhanced Combustion Behavior. *Chem. Eng. J.* **2020**, *395*, 125114.